# VISUALIZATION OF FLUID FLOWS USING THE HYDROGEN-BUBBLE TECHNIQUE

**Ittichote Chuckpaiwong, Sukit Wansophonkul,**

**Traiwit Wongaphiwattanakul and Asi Bunyajitradulya**

*Fluid Mechanics Research Laboratory, Department of Mechanical Engineering,*

*Faculty of Engineering, Chulalongkorn University, Bangkok 10330, Thailand*

**ABSTRACT**

The hydrogen-bubble technique for visualizing fluid flow was investigated. A simple setup was designed, tested, and employed in the studies of flow past a flat plate and wake of a cylinder. The setup proved effective for studying the physics of these flows, at low Reynolds number. Particularly, edge separation, fluid deformation, entrainment mechanism, Karman's vortex street, and vortex shedding were observed. The paper describes in detail the setup and the techniques ranging from the water channel, the electronics, the suitable lighting condition, and the imaging.

## 1. INTRODUCTION

Flow visualization is one of the most powerful tool for studying fluid flow phenomena. In early years, it was most commonly used as a means to study, qualitatively, flow fields and the underlying physical processes. Some of the earlier but still commonly used techniques are the hydrogen-bubble, the smoke-wire, the tuft, the shadowgraph, and the Schlieren techniques. To cite but a few of works that employed these techniques are the studies of boundary layers using the hydrogen-bubble technique by Geller (1995) and Kline et al. (1976), of turbulent flows using the smoke-wire technique by Nagib (1979), of a transverse jet using the smoke-wire technique by Fric and Roshko (1994), of flow behind wings using the tuft grid technique by Bird (1952), of incompressible turbulent shear layers using the shadowgraph technique by Brown and Roshko (1974), and of compressible turbulent shear layers using the Schlieren technique by Papamoschou and Roshko (1988).

With the advent of the laser and the CCD camera technologies during the past two

decades, however, most of the recent and more advanced flow visualization techniques are based on some form of laser diagnostics. Examples are the Planar Laser-Induced Fluorescence (PLIF), the Planar Laser Rayleigh Scattering (PLRS), and the Planar Laser Mie Scattering (PLMS) techniques. These techniques do not give only visual images of the flow, but they also give quantitative information on properties of the flow field. Some of the recent works that employed these techniques are the studies of compressible shear layers using the PLIF technique by Bunyajitradulya and Papamoschou (1994), and Papamoschou and Bunyajitradulya (1997); of compressible boundary layers using the PLRS technique by Smith et al. (1989); and of compressible shear layers using the PLMS technique by Clemens and Mungal (1991), and Fourguette et al. (1990).

This paper describes a simple setup which employs the hydrogen-bubble technique in visualizing flow fields. The setup can be made quite easily from common electronic components but can be applied rather effectively in the study of physics of fluid flows at low Reynolds number. Examples of the flow studied are flow past a flat plate and wake of a cylinder.

## 2. THE HYDROGEN-BUBBLE SETUP AND FLOW FACILITY

Most fluids are transparent media, and their motion cannot be observed directly with the human eye. Some means must therefore be employed to make the flow visible. One of the methods commonly used in this regard is the introduction of foreign materials, generally referred to as *tracers*, into the flow. For best result the tracer used should have high visibility as well as the ability to follow faithfully local velocity of the flow.

The hydrogen-bubble technique has proven quite effective for visualizing fluid flows at low Reynolds number. The technique employs the principle of electrolysis of water to generate hydrogen bubbles. It is well known that, if a dc voltage is applied between two electrodes in water, hydrogen bubbles are formed at the cathode and oxygen bubbles at the anode. Generally, either the hydrogen bubbles or the oxygen bubbles can be used as tracers. However, because the hydrogen bubbles formed at the cathode are much smaller than the oxygen bubbles at the anode, they can follow local fluid velocities more faithfully and, therefore, are chosen as tracers.

Figure 1 illustrates the schematic diagram of the setup. The experiments were conducted in the Fluid Mechanics Research Laboratory (FMRL), Department of Mechanical Engineering, Chulalongkorn University. The facility used is a 46 x 120 $cm^2$ water bed driven by a one hp pump. The water bed is equipped with a flow control valve and a flow meter for flowrate adjustment and measurement respectively. Before entering the test bed, water from the pump is conditioned in the settling chamber by a common household

screen (15 mesh per inch), three layers of marbles, and another household screen. The layers of marbles are used to remove large-scale fluctuations and swirls, which certainly exist in a pipe downstream of a flow meter, while the second screen after the marbles is used to remove the remaining small-scale fluctuations. Additional screens with finer mesh can be added to further remove small-scale fluctuations, if required. After conditioned, the flow of water entering the test bed is reasonably free of disturbances. The water level in the test bed can be adjusted by stacking up a number of metal bars (each approximately 7 mm thick) at down-stream location. Besides being used as a level control, the metal bars are also used as an anode. In this experiment, the water level

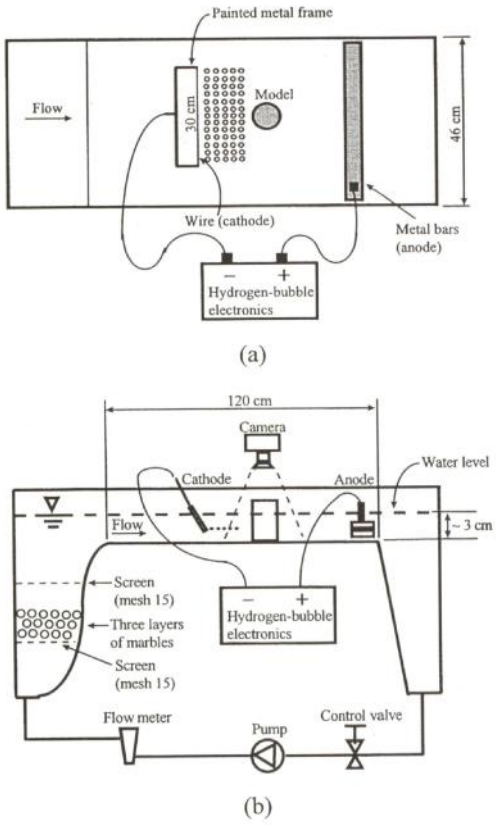


**Fig. 1 Schematic diagram of the setup: (a) top view; (b) side view.**

was kept at approximately 3 cm high and the speed was set at approximately 2 cm/s.

To generate hydrogen bubbles, a circuit in Fig. 2 was used. The first section of the circuit is a full-wave rectifier with an input from a variac. The output of the rectifier is a dc voltage which can be varied between 0-220 V. The second section of the circuit is a manual/ext.-trigger mode selection. In manual mode, switch $S_2$ is used. In external trigger mode, switch $S_3$ is connected to a BNC, and an external signal can then be applied at the BNC to control/time the voltage applied to the electrodes. in this case, if a function generator is used, steady and adjustable timelines can be generated. Finally, switch $S_4$ is used for inverting the polarity of the electrodes. This is to prevent deposition of metal oxide at the anode. The voltage used in this experiment ranged between 150 to 200 V.

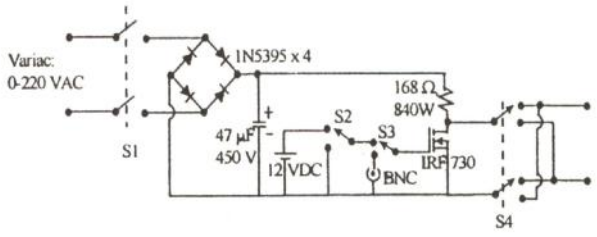


**Fig. 2 Electronic circuit used to generate hydrogen bubbles.**

The cathode used in this experiment was an ordinary electrical wire, 0.16 mm in diameter. To get a sheet of bubbles wide enough to cover the span of a model, the electrical wire of 30 cm long was stretched across a metal frame, see Fig. 3a. Since part

of the metal frame was unavoidably submerged in water, it could generate unwanted disturbance. To minimize this disturbance, the frame was made of a thin rod of 2 mm in diameter. In addition, the submerged part of the frame was painted to prevent bubble generation. Fig. 3b illustrates the positioning of the cathode.

To increase the conductivity level of the water, therefore improve bubble generation, salt (NaC1) was dissolved into the water. The suitable concentration was found to be approximately 0.4% by mass.

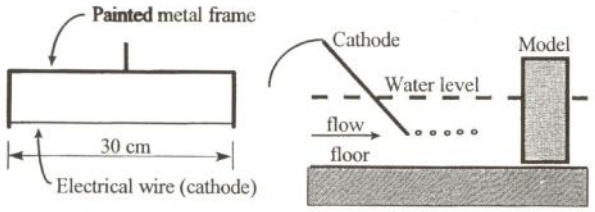


**Fig. 3 (a) The cathode; (b) the positioning of the cathode (side view).**

Lighting is crucial in imaging of flow fields, particularly at low source level. For good contrast, background light (any light that does not come directly from the subject, i.e., the hydrogen bubbles) should be eliminated as much as possible. Consequently, the floor of the test bed was painted black and the imaging was done in a darkroom, constructed from a frame and black curtains. If available, a CCD camera should be used for interactive photography session. In our case, a 35 mm SLR camera (Minolta 7000i) with a close-up lens was used. The light source was a 50 W halogen lamp arranged in a manner illustrated in Fig. 4. Because of reflection, a flash attached to a camera is unsuitable. For the lighting condition used and the shutter speed required in our case (1/4 at f/3.5), ISO800 films have proven sufficient. Focusing was done by placing a target at the same height as that of the bubbles, i.e., the height of the electrode wire.

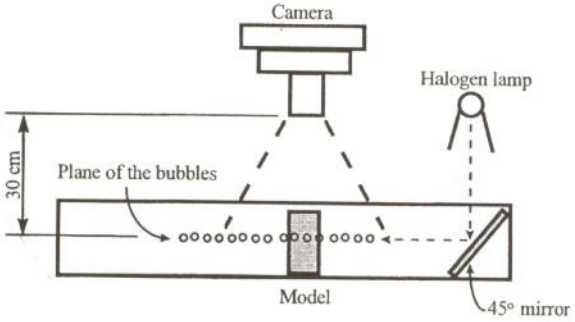


**Fig. 4 Arrangement and positioning of the model, the light source, and the camera (end view).**

Finally, the shutter speed chosen (in relation to the flow speed) has direct effect on the kind of image acquired. For fast shutter speed, the hydrogen bubbles are seen as discrete elements (Fig. 5a); for medium shutter speed, as discrete segments of lines which are traces of the bubbles (Fig. 5b); for slow shutter speed, as continuous lines which are average paths (Fig. 5c).

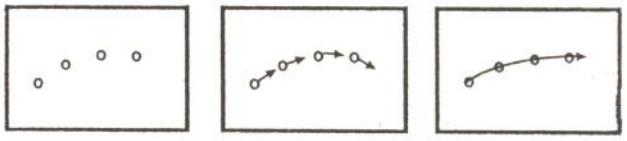

(a) (b) (c)

**Fig. 5 The kind of image acquired depends upon the shutter speed (in relation to the flow speed): (a) fast shutter speed; (b) medium shutter speed; (c) slow shutter speed.**

For further detail of the setup, see Chuckpaiwong et al. (1998).

## 3. RESULTS AND DISCUSSION

In all images shown below, the flow is from left to right; the freestream velocity is approximately 2 cm/s; the bright vertical line on the left is the electrode, where the hydrogen bubbles are generated; and the field of view is approximately 9 cm wide and 13 cm long.

### 3.1. Flow past a flat plate

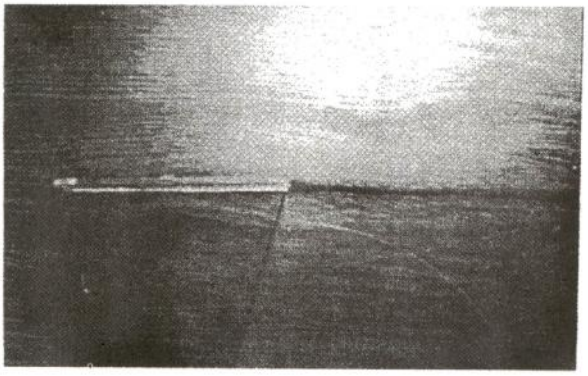

**Image 1** ***Flow past a flat plate at zero angle of attack.*** This image illustrates flow pattern around a flat plate at zero angle of attack. Due to long exposure, discrete hydrogen bubbles are not seen. Instead, what captured are traces of the bubbles, which are seen as alternating bright thin lines. These lines are the approximate of instantaneous streamlines. In this case, the flow passes the plate smoothly without separation.

Condition : *Re* based on chord length ~ 1000, exposure time ~ 0.25 s.

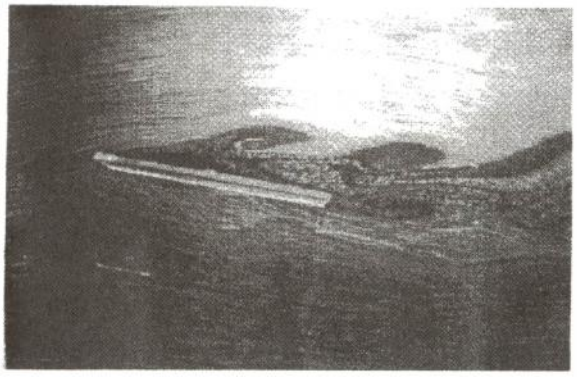

**Image 2** ***Flow past a 15-degree inclined flat plate.*** In contrast to Image 1, separation at the leading edge is apparent in this image. Vortex shedding occurs both at the leading and the trailing edges. At the leading edge, the resulting vortices rotate clockwise, and at the trailing edge, counter-clockwise. As a result of the shedding of these vortices, the pressure distribution on the surfaces of the plate varies in a periodic manner, causing a periodic resultant force on the plate. In this case, the shedding frequency is approximately 0.7 Hz.

Condition : *Re* based on chord length ~ 1000, exposure time ~ 0.25 s.

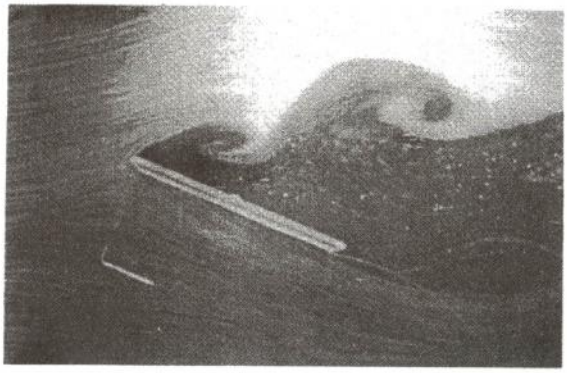

**(3a)**

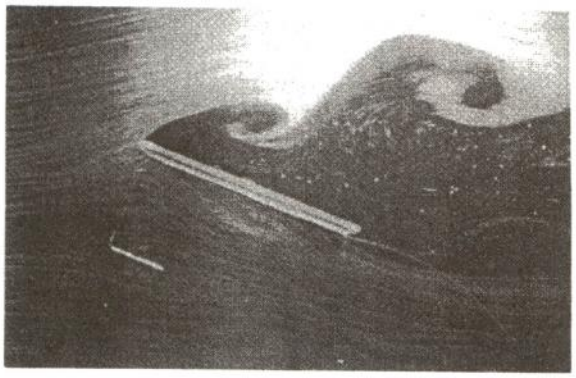

(3b)

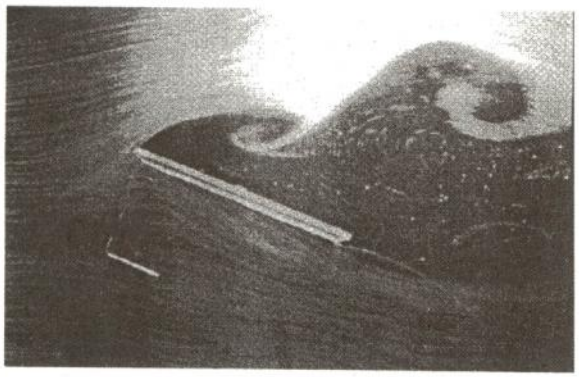

(3c)

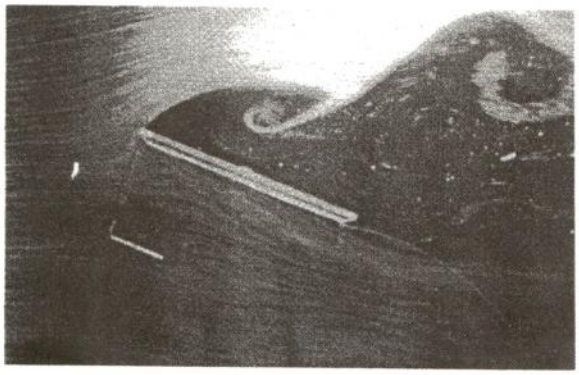

(3d)

**Image 3a-d** ***Flow past a 30-degree inclined flat plate.*** This set of images was taken sequentially, starting from Image 3a and ending in Image 3d, with time delay between consecutive images of approximately 0.5 *s*. Of interest in this set of images is the deformation of fluid elements, illustrated in Fig. 6. The fluid elements along the braid (the region connecting two vortical structures) are stretched in the *x*-direction and compressed in the *y*-direction. In these images, the braid region, which looks like 'an elephant trunk,' is seen as being stretched along the line connecting the two structures. Also, of interest is the *entrainment* of freestream fluid due to vortex *roll-up*, illustrated in Fig. 6. As adjacent vortices roll up, they create a streamline pattern in the braid region such that freestream fluid is entrained, sheared and then mixed at the vortex cores. See Dimotakis (1986) for further details. Condition : *Re* based on chord length ~ 1000, exposure time ~ 0.25 s.

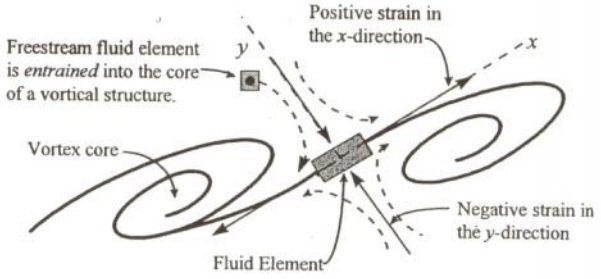


**Fig. 6 Flow pattern in the braid region between two vortical structures.**

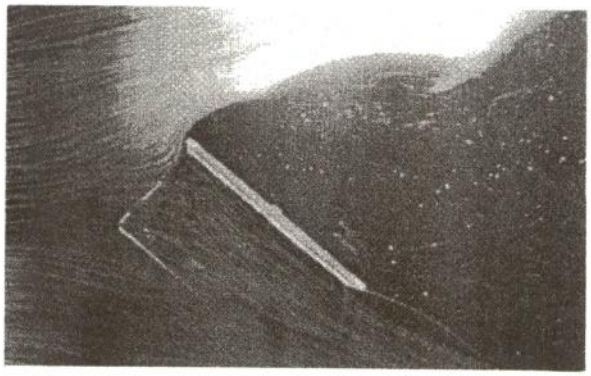

**Image 4** ***Flow past a 45-degree inclined flat plate.*** Compared with the flows in Images 2 and 3a-d, the roll-up of vortices in this image is less obvious. What is more obvious is the shifting of a stagnation point down the lower surface of the plate as illustrated in Fig. 7. Condition : *Re* based on chord length ~ 1000, exposure time ~ 0.25 s.

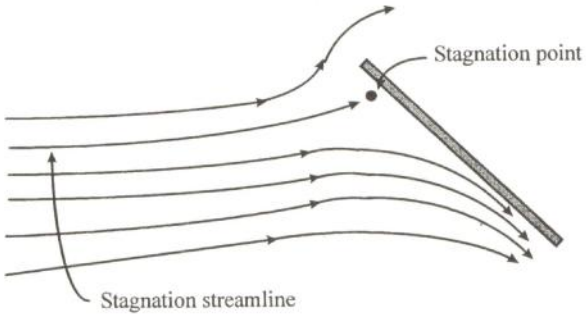


**Fig. 7 Stagnation point flow near the leading edge of an inclined flat plate.**

### 3.2 Wake of a cylinder

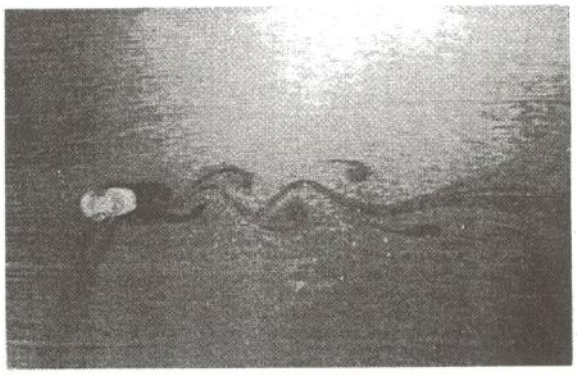

**Image 5** ***Cylinder diameter = 8 mm.*** This image shows the flow regime which is known as *Karman's vortex street.* It is the regime in which discrete vortices can be seen shedding alternately from both sides of a cylinder. As a result of this vortex shedding, pressure distribution on the surface of a cylinder varies periodically, causing a cyclic-force loading on the cylinder. In this case, the shedding frequency was measured to be 1 Hz.

Condition : ***Re*** **~ 200, exposure time ~ 0.25 s.**

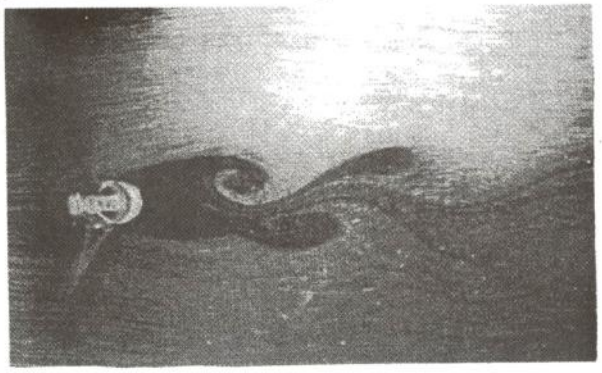

**(6a)**

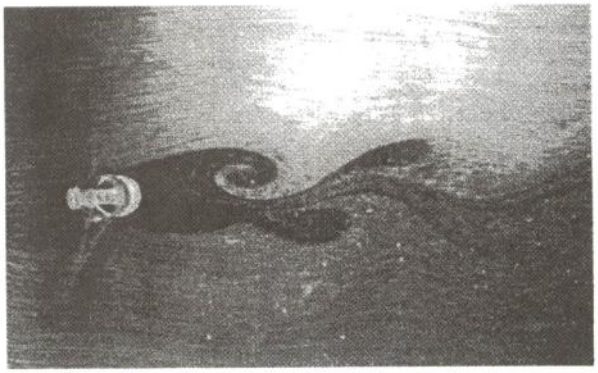

**(6b)**

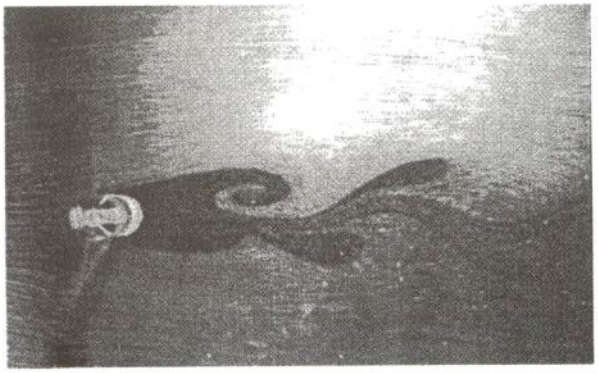

**(6c)**

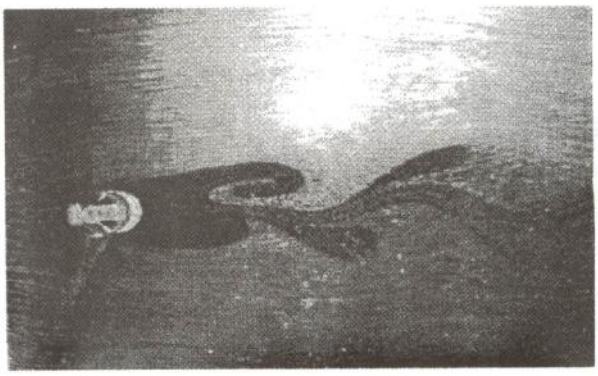

**(6d)**

**Image 6a-d** ***Cylinder diameter = 13 mm.*** This set of images was taken sequentially, with time delay between consecutive images of approximately 0.5 *s.* Again, the stretching of 'an elephant truck,' starting from Image 6a to Image 6d, is pronounced.

Condition : *Re* ~ 325, exposure time ~ 0.25 s.

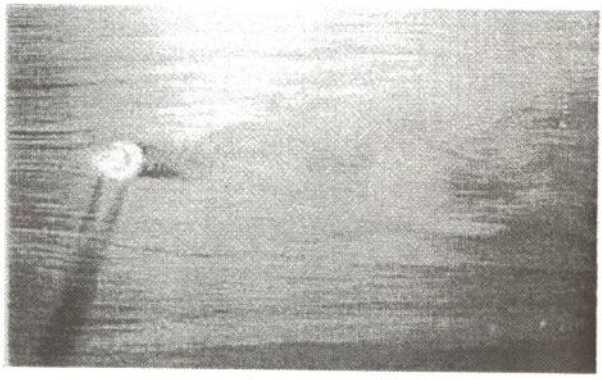

**Image 7** ***Cylinder diameter = 8 mm.*** The flow condition in this image is the same as that of Image 5. The shutter speed used, however, is slower. Hence, the bubbles appear as continuous traces.

Condition: *Re* ~ 200, exposure time ~ 0.5 s.

## 4. CONCLUSION

The hydrogen-bubble technique has proven effective for studying fluid flows at low Reynolds number. Physical processes relevant to the flows studied, particularly, edge separation, deformation, entrainment, Karman's vortex street, and vortex shedding were observed.

At this point, it is insightful to compare the technique with other simple techniques such as the smoke-wire and the tuft techniques. But before a comparison can be made, one has to keep in mind that different technique employs different physical mechanism in bringing out features of the flow. Therefore, the comparison can be made only as far as the applicability of the techniques in the flow of interest. For example, since the hydrogen-bubble technique employs the principle of electrolysis of water, it is obviously not applicable in air flows. In contrast, the smoke-wire technique relies on high concentration streaks of oil fog, it is therefore not applicable in water flows. (See Rassame et al. 1998 for details on the smoke-wire technique.) In addition, because of the difference in physical mechanism employed, one has to take into account the difference in the end result. For the hydrogen-bubble and the smoke-wire techniques, the end result is streakline; for the tuft technique, directed tuft. (For the definition of streakline, see for example Fox and McDonald 1978.) With these in mind, one may say that the hydrogen-bubble technique has several advantages over the smoke-wire and the tuft techniques. Specifically, compared with the smoke-wire technique, the hydrogen-bubble technique is easier to set up and the visualization can be done continuously. Compared with the tuft technique, the hydrogen-bubble technique gives more details of the flow due to higher spatial resolution (defined in terms of minimum spatial separation between two distinguishable tracers.)

Finally, because of the random dispersion of bubbles associated with turbulent fluctuation, it should be noted that the technique is not suitable for high Reynolds number flows.

## 5. REFERENCES


1. Bird, J., (1952), "Visualization of flow fields by use of a tuft grid technique," *J. Aero. Sci.*, July 1952, pp. 481-485.
2. Brown, G. L. and Roshko, A., (1974), "On density effects and large structure in turbulent mixing layers," *J. Fluid*

*Mech.,* Vol. 64, pp. 775-816.

3. Bunyajitradulya, A. and Papamoschou, D., (1994), "Acetone PLIF imaging of turbulent shear-layer structure at high convective Mach number," AIAA Paper No. 94-0617.
4. Chuckpaiwong, I., Wansophonkul, S., Wongaphiwattanakul, T. and Bunyajitradulya, A., (1998), "Fluid flow studies using flow visualization: The hydrogen-bubble technique," FMRL Report No. 2103-499/1, Fluid Mechanics Research Laboratory, Department of Mechanical Engineering, Chulalongkorn University.
5. Clemens, N.T. and Mungal, M.G., (1991), "A planar Mie scattering technique for visualizing supersonic mixing flows," *Exp. in Fluids,* Vol. 11, pp. 175-185.
6. Dimotakis, P.E., (1986), "Two-dimensional shear-layer entrainment," *AIAA Journal,* Vol. 24, No. 11, pp. 1791-1796.
7. Fourguette, D.C., Mungal, M.G. and Dibble, R.W., (1990), "Time evolution of the shear layer of a supersonic axisymmetric jet at matched conditions," AIAA Paper No. 90-0508.
8. Fox, R. W. and McDonald, A.T., (1978), Introduction to Fluid Mechanics, 2nd edition, John Wiley & Sons, New York.
9. Fric, T. F. and Roshko, A., (1994), "Vortical structure in the wake of a transverse jet," *J. Fluid Mech.,* Vol. 279, pp. 1-47.
10. Geller, E. W., (1955), "An electrochemical method of visualizing the boundary layer," *J. Aero. Sci.,* Vol. 22, pp. 869-870.
11. Kline, S.J., Reynolds, W. C., Schraub, F. A. and Runstadler, P. W., (1976), "The structure of turbulent boundary layers," *J. Fluid Mech.,* Vol. 30, pp. 741-773.
12. Nagib, H. M., (1979), "Visualization of turbulent and complex flows using controlled sheets of smoke streaklines," in *Flow Visualization,* Asanuma, T. Editor, pp. 257-263, Hemisphere, Washington, D.C.
13. Papamoschou, D. and Bunyajitradulya, A., (1997), "Evolution of large eddies in compressible shear layers," *Phys. Fluids,* Vol. 9, No. 3, pp. 756-765.
14. Papamoschou, D. and Roshko, A., (1988), "The compressible turbulent shear layer: an experimental study," *J. Fluid Mech.,* Vol. 197, pp. 453-477.
15. Rassame, S., Siripoorikan, B., Buensawang, S., Petitanalap, Y. and Bunyajitradulya, A., (1998), "Visualization of Fluid Flows Using The Smoke-Wire Technique," submitted to the *Research and Development Journal of The Engineering Institute of Thailand* for publication.
16. Smith, M., Smits, A. and Miles, R., (1989), "Compressible boundary-layer density cross sections by UV Rayleigh scattering," *Optics Letters,* Vol. 14, No. 17, pp. 916-918.